Nuclear Inst. and Methods in Physics Research, A 1039 (2022) 166927

Contents lists available at ScienceDirect

Nuclear Inst. and Methods in Physics Research, A

journal homepage: www.elsevier.com/locate/nima

Radiation effects induced by the energetic protons in 8x8x32 mm3 CdZnTe detectors

A. Bolotnikov [a,*], G. Carini [a], M. Chekhlov [a], A. Dellapenna [a], J. Fried [a], J. Haupt [a], S. Herrmann [a], I. Kotov [a], D. Medvedev [a], A. Moiseev [b,c], G. Pinaroli [a], A. Rusek [a], M. Sasaki [b,c], M. Sivertz [a], L. Smith [b], E. Yates [b]

[a] Brookhaven National Laboratory, Upton, NY 11793, USA
[b] University of Maryland, College Park, MD 20742, USA
[c] CRESST/NASA/Goddard Space Flight Center, Greenbelt, MD 20771, USA

ARTICLE INFO

Keywords:
CdZnTe detectors
Radiation effects
Radiation damage
Gamma ray imaging

ABSTRACT

CdZnTe (CZT) detectors have been used in the past and are being actively considered for future gamma-ray space telescopes. One of the challenges of operating CZT detectors in low Earth orbit is radiation damage caused by energetic protons. Previous studies concluded that fluences of 10^8 -10^9 p/cm^2 are sufficient to cause shifting of peak positions and degradations of energy resolution. Degradation of detectors after proton irradiation has been extensively investigated to determine their radiation resistance limits and performance recovering procedures for their applications in space and nuclear nonproliferation. Here we present the study of radiation effects induced by 100 MeV protons in 3-cm long CdZnTe detectors that we recently proposed for the gamma-ray telescope GECCO. The goal of this study is to evaluate the feasibility of using such long CZT detectors in future space missions.

1. Introduction

Over the past decade, CdZnTe (CZT) gamma-ray detectors have been increasingly used in a broad area of applications including space, medical imaging, and nuclear nonproliferation with a growing trend of employing thicker and bigger detectors with extended energy range and ability to accurately measure the location of interaction points. For practical applications, the thickness of the CZT detectors is always a tradeoff between required performance and cost/availability of CZT crystals. In the past, CZT detectors with thickness of a few millimeters were the only option for making gamma-ray space telescopes. Today, high-quality CZT crystals with thicknesses up to several centimeters can be obtained from commercial suppliers.

Arrays of the bar-shaped CZT detectors with thickness up to 35 mm and cross-sections up to 10 × 10 mm^2 have been considered for two future gamma-ray telescopes: AMEGO [1] and GECCO [2]. Such bars, configurated as position-sensitive virtual Frisch-grid (or capacitive Frisch-grid) detectors, offer an economical way of integrating large effective area detecting planes for coded aperture or Compton telescopes, which opens an opportunity for developing new telescopes for measuring galactic gamma rays in the MeV energy range—the least explored energy band today [3]. A potential challenge of using such detectors is long electron collection times, up to 3 μs, which may result in polarization effects, particularly in the presence of large radiation backgrounds in space.

Satellites operating in a Low Earth Orbit (LEO) pass daily through the South Atlantic Anomaly radiation belt where the onboard instruments are exposed to high fluxes of highly-ionizing non-relativistic protons. The cumulative effect over years of operation degrades the detector performance and causes nuclear line activations [4–10]. The equatorial low-Earth orbits help to minimize these effects but cannot eliminate them. The models (we refer here to the most recent review [10]), predict that the total proton fluence, which depends on the orbit's inclination and altitude, are of ~2 × 10^9 p/cm^2/year.

Performance degradations of CZT detectors after exposure to high fluxes of radiation have been extensively investigated to determine their tolerance limits to different types of radiation in instruments used in a variety of fields, including space and nuclear nonproliferation. For example, the early measurements, summarized in [5,6], indicated that detectors exposure to 10^{12} p/cm^2 1.3 MeV protons caused significant increases of leakage currents, while gradual peak shifts and energy resolution degradation following 200 MeV proton irradiation were observed starting at ~10^8p/cm^2. The comprehensive studies of CZT and CdTe detector activation in LEO including measurements of the proton induced gamma-ray lines were carried out by several groups, e.g., [7,8]. Spectral degradation of 2-mm detectors was observed in [8] after an

* Corresponding author.
E-mail address: bolotnik@bnl.gov (A. Bolotnikov).

https://doi.org/10.1016/j.nima.2022.166927
Received 26 March 2022; Received in revised form 14 May 2022; Accepted 16 May 2022
Available online 9 June 2022
0168-9002/Published by Elsevier B.V.

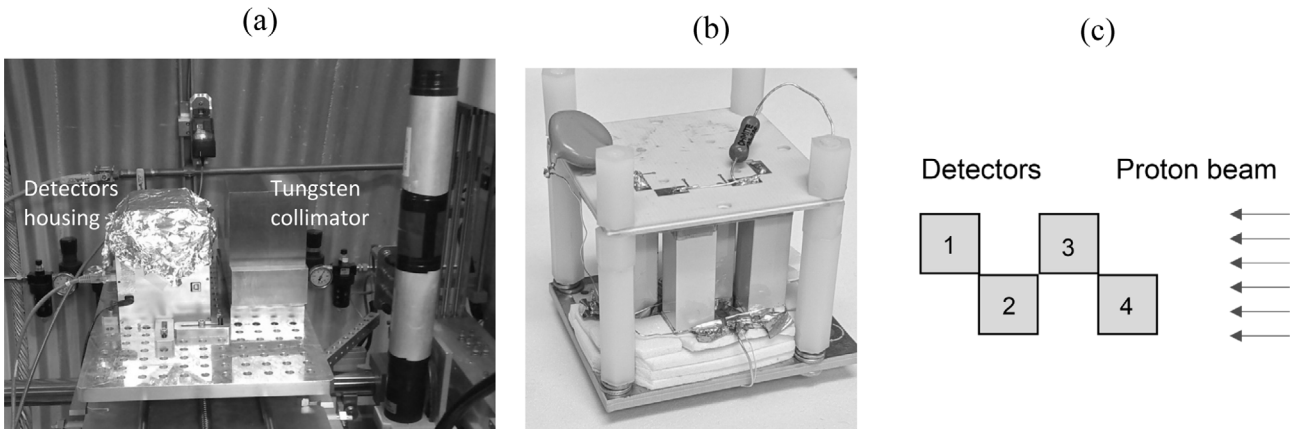

Fig. 1. (a) Test box with detectors and readout electronics installed inside the target room; (b) 4 8 × 8 × 32 mm^3 detectors mounted on the fanout board; (c) positions of the detectors with respect to the beam.

accumulated proton fluence of 4.5 × 10^{10} p/cm^2, while for the ~1 mm CdTe detectors no degradation was found up to the maximum fluence of 2.5 × 10^9 p/cm^2 used in these measurements.

CZT detectors have been successfully flown in a number space missions, and the radiation-related effects induced by cosmic radiation have been rigorously investigated. However, the thicknesses of the detectors used in previous experiments were limited by several millimeters, while the long CZT detectors are expected to be more susceptible to polarization effects and radiation damage, caused by the trapped protons in low Earth orbits.

Here, we present studies of the radiation effects in 8x8x32 mm^3 CdZnTe detectors, carried out at the NASA Space Radiation Laboratory employing the high-energy proton beam extracted from the BNL accelerator.

2. Experimental

The measurements were carried out at the NASA Space Radiation Laboratory (NSRL) established to provide charged particle beams for space radiation research [11]. We employed the proton beam with energies of 100 and 150 MeV to irradiate 4 8 × 8 × 32 mm^3 CZT detectors. The beam aperture of 4 × 5 cm^2 is defined by thick tungsten blocks to minimize exposure of the readout system's mechanical components. Fig. 1(a) shows a picture of the aluminum test box, housing the detectors and electronics, mounted with the proton beam entering the detectors from the right side. It also shows the tungsten blocks (on the right from the test box) and gas ionization chamber for monitoring proton rates. The proton beam irradiated all the volume of the detectors. The time beam profile has a period of 4 s with protons uniformly distributed in time during a ~4 s spill, followed by a ~3.6 s beam-off time. The maximum beam intensity is ~10^{11} protons per spill.

2.1. CZT detectors and readout electronics

For these studies, we fabricated 4 virtual Frisch-grid detectors using 8x8x32 mm^3 CZT crystals acquired from Redlen [12]. The detectors were mounted vertically on the fanout board by gently pressing them from the top with the cathode board as illustrated in Fig. 1(b). The detector positions with respect to the proton beam are schematically shown in Fig. 1(c). The analog frontend AVG ASIC [13] was bonded to the opposite side of the fanout board that also had two multi-pin connectors. The cathode board carried a decoupling capacitor to read signals from the detector cathodes which were interconnected together via the cathode board. The whole assembly was plugged into the readout motherboard inside the aluminum enclosure with USB and power cables. For each interaction event, the readout ASIC captured the anode and cathode signal amplitudes and sent them for off-line analysis. The cathode signals were used to measure locations of interaction sites along the detector length and apply the interaction depths corrections. The detectors and readout electronics were calibrated using an uncollimated ^{137}Cs source after installing the system in the beam right before the measurements. The calibration included finding the baselines and dependencies of the anode amplitudes on the cathode to anode ratios (A vs. C/A) required for the interaction depth (1D) corrections. The detectors were biases at 3700 V, which corresponded ~3.3 μs drift time in 32 mm long CZT detectors. The ASIC amplifiers peaking time was selected to be 3.5 μs.

For the electron lifetime measurements before and after detector exposure, we used a different readout approach based on sampling of the charge signals captured with the hybrid 1-ms decay time eV-preamplifiers [13,14]. The waveforms sampling allowed us to accurately measure the dependence of the collected charge on the drift time for the events interacting near the cathode at different biases. The later conditions are important to minimize the effect of the holes. Fitting these dependences allowed us to estimate the electron life times.

2.2. Experimental procedure

The measurements were conducted in two days. In the first day, we used 150-MeV protons fluxes like those expected in LEO, to investigate the potential polarization effects. The detector responses were continuously monitored by measuring the 511-keV background line and gamma rays from a ^{137}Cs source placed on the top of the test box. Every 30 min the intensity of the beam was increased, however the total accumulated fluence was kept below the level at which the response degradations due to radiation damage are expected. At these conditions, photopeak shifts would indicate the polarization effect that could be also verified by shutting down the proton beam and observing the recovery of the peak positions.

It is important to mentioned that we calibrated the detectors in the beginning of each day (before the irradiations) and used the same calibration parameters (gains, and A vs. A/C curves) to plot the acquired spectra.

During the second day, we employed 100-MeV protons with much higher fluxes to investigate detector response degradations caused by radiation. Before taking measurements, we remeasured the initial peak positions using the 662-keV photons for the ^{137}Cs source. The detectors were irradiated for 15 min followed by ~15 min cooldown during which we monitored the detector responses by measuring the pulse-height spectra using the 511 and 662-keV lines. Using NIST tables, we estimated that a 100-MeV proton deposits energy of ~22 MeV in the front two bars and ~28 MeV in the shielded bars, as shown in Fig. 1(c). The deposited charges saturated the readout electronics for a spill duration plus some recovery time, but we still were able to

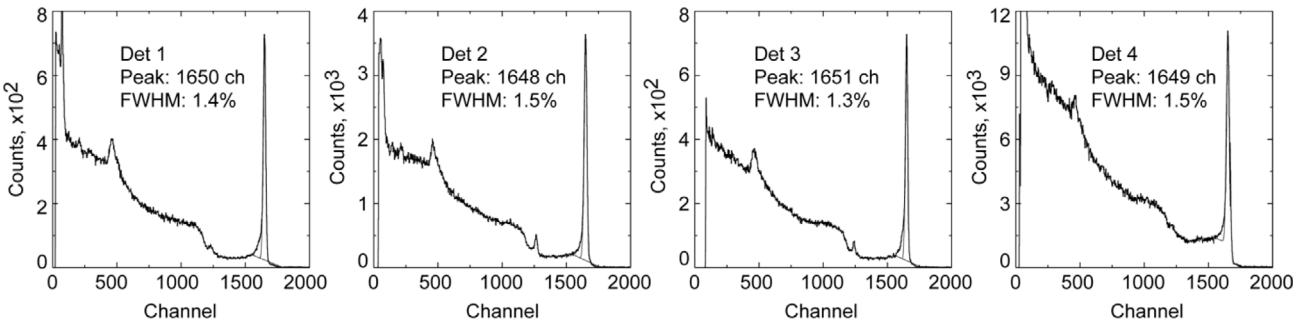

Fig. 2. Initial 1D corrected spectra measured for all 4 detectors from ^{137}Cs at the temperature of ~23 degree C inside the target room before irradiation. All detectors show good performance with energy resolutions of 1.3-1.5% (FWHM at 662 keV).

measure the 511 and 662-keV photopeaks even during the irradiation. Increasing the proton fluxes in each run, we eventually observed small shifts of the peak positions, indicating a decrease of the electron lifetime. After a total fluence of 4×10^7 p/cm^2 or ~10^8 protons per detector, which is comparable to the fluences expected in equatorial LEO over a 5-year mission, the photopeak positions shifted ~2%. At the end of the measurements, the detectors were irradiated for ~30 min using the maximum proton rate with a total fluence of ~10^{10} p/cm^2. Our goal was to monitor the detector performance degradation in real time. Unfortunately, during the measurements the readout system stopped responding after ~2 min of irradiation due to ASIC latching. The readout system was not designed for remote power control. After completing the irradiation and shutting down the beam, we entered the target room and restarted the readout system, which started functioning normally, however the detectors showed no responses.

Although the detectors became activated, their internal backgrounds after 2 weeks of cool-down became acceptably low to continue our studies. After removing the detectors from the test box, we measured the internal background spectra using a high-purity Ge detector (ORTEC Solid-State Photon Detector, GEM30P4-83) and with CZT detectors themselves after annealing was carried out to recover their performance. During the following months, we were monitoring detector responses and measured a reduction in their internal backgrounds. After a year, the internal background was practically invisible in comparison to the natural background in the lab.

We carried out 2 annealing runs in dry conditions at 65 and 80 degree C for 3 weeks each run without removing detectors from the fanout board. After each annealing, the detectors were plugged back into the readout system and continuously tested for several months. In ~10 months we repeated the second annealing at 80 degree C for 3 weeks and observed further improvement of the detector responses.

3. Results and discussions

The detectors were characterized before the proton exposure with the final calibrations done inside the target room. Fig. 2 shows the pulse-height spectra measured from all the detectors using the uncollimated ^{137}Cs source at the temperature of ~23 degree C inside the target room. Three detectors out of four showed exceptional performance with energy resolutions of 1.3-1.5% (FWHM at 662 keV) after 1D corrections and 3%–4% before corrections. The fourth detector had a higher background in the Compton continuum region and lower peak to Compton edge ratio, likely due to the sub-grain boundary that effected uniformity of the charge collection in the crystal. This detector would not be used in practical instruments, but it is well suitable for these studies. The low energy lines from the activation background in the target room, along with the 511-keV line, are seen in the spectra. The electron lifetime measured for these detectors using the waveforms sampling readout [12,13] were found to be 80, 81, 78, and 60 μs, respectively. The initial correction parameters were used to plot the spectra after irradiation.

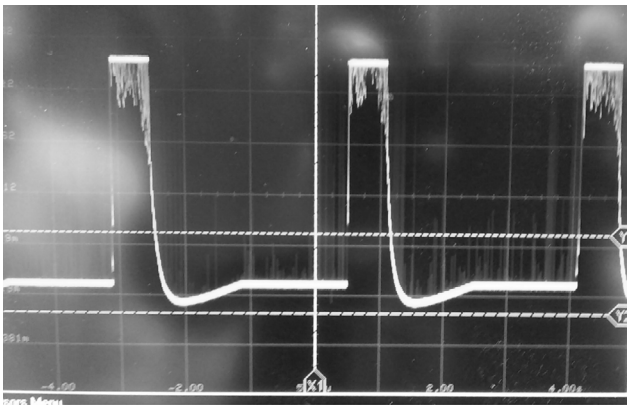

Fig. 3. A photograph of the oscilloscope's screen with a bright curve representing of the overlapping signals generated by ^{137}Cs gamma rays and proton spills. As seen, the readout electronic is saturated when the beam is "on" and when the beam is "off", detector can continue capturing the ^{137}Cs signals. The individual gamma-ray interaction events (faded vertical lines) are seen between the proton spills. The time scale is 1 s.

We continuously monitored output signals coming from the detectors with an oscilloscope. As an example, Fig. 3 shows a photograph of the oscilloscope's screen with the bright curve representing overlapping baselines of the signals generated by the ^{137}Cs gamma rays. During the spills, proton events saturated the readout electronics with the baseline going up in the screen. At the end of the spill, the baseline moved below its original position before a full recovery. Individual pulses from gamma ray interactions are seen as vertical lines between the proton spills, which means that we could monitor the photopeak positional shifts in the pulse-height spectra during the irradiation runs. As the number of protons per spill increased it took longer for the readout system to recover, while the normal baseline position time intervals became shorter. Effectively, it increased the system dead time. But even at the highest rate used in these measurements (3×10^7 p/cm^2/spill), we were able to distinguish the photopeaks in the pulse height-spectra. Similar system behavior would be expected when a satellite passes through the South Atlantic Anomaly.

3.1. Low-flux measurements

We used the 150 MeV protons with fluxes up to 160 p/cm^2/s to investigate polarization effects in 3-cm thick CZT detectors that may occur when the detectors operate in LEO with typical proton fluxes of ~2 p/cm^2/s. Each 160-MeV proton crossing a CZT bar deposited ~20 MeV energy and saturated the readout electronics, but still, no polarization was observed in our detectors up to a maximum flux of 160 p/cm^2/s. Fig. 4 shows relative 662-keV peak positions evaluated for all four detectors at different proton fluxes. The spectra were collected during the proton irradiations. These results demonstrated

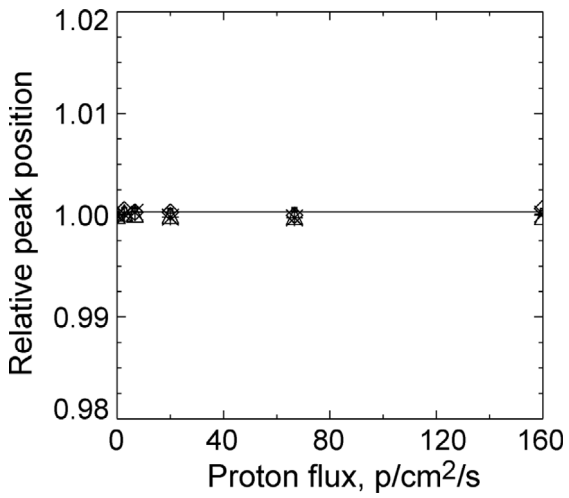

Fig. 4. Relative 662-keV photopeak positions evaluated for 3-cm drift CZT detectors at different proton fluxes. The spectra were collected during the proton irradiations.

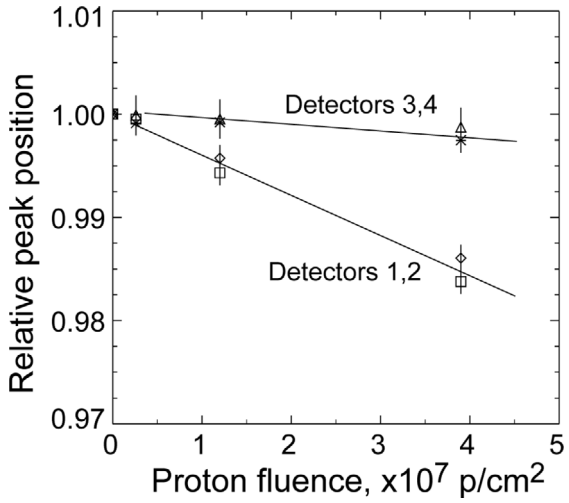

Fig. 5. Detector response degradations of the 3-cm drift CZT detectors due to radiation damage caused by 100 MeV protons. Detectors 1 and 2, which were behind the front Detectors 3 and 4, exhibit stronger radiation damage.

that 3-cm drift CZT detectors will not suffer from polarization effects while operating in LEO. This was previously concluded by other teams for thinner CZT detectors [6,7].

3.2. High flux measurements

Here, we studied the detector response degradation due to radiation damage by irradiating the detectors with 100-MeV protons. Each 30 min irradiation run was followed by a 30 min cool-down time during which we collected spectra from the ^{137}Cs check source and external activation 511-keV line. No changes in peak positions were observed up to a fluence of 10^6 p/cm^2. While continuing to increase the proton exposure up to 4×10^7 p/cm^2 or ~10^8 protons per detector, we observed small (<2%) shifts in the peak positions, indicating a small decrease of the electron lifetime (Fig. 5), which can be corrected using in orbit calibrations. As seen, detectors 1 and 2, which were behind the front detectors 3 and 4, exhibit stronger radiation damage because 100 MeV protons deposited more energy in the back detectors. The measurements reported in [7,8] also demonstrate that there are practically no changes of the electron lifetimes up to a proton fluence of 10^8 p/cm^2—such doses are expected for a 5-year mission.

Fig. 6. shows pulse-height spectra measured inside the target room after the detectors received a proton fluence of 10^7 p/cm^2. The spectra were collected between two irradiation runs for 15 min. Most of the lines seen in the spectra are from the external activation, i.e., high Z materials surrounding the test box. The internally activated background in CZT contributes to the low energies below 200 keV.

At the end of the measurements, we exposed the detectors to an extremely high proton flux for ~30 min with a total fluence of 9×10^9 p/cm^2. Since the readout electronics stopped responding after 2 min of irradiation, we were unable to monitor the detector responses during the run. After completing the irradiation and shutting the beam down we restarted the readout system which continued to operate normally. Unfortunately, the detectors suffered from radiation damage and showed no signals above the noise level, which remained unchanged. We did not take *I-V* measurements after irradiation but, based on the electronic noise, we could conclude that the leakage current has not changed. The initial leakage currents measured for these detectors were <10 nA at 3700 V. The signals disappearance can be entirely attributed to decay of the CZT electron lifetime.

3.3. Induced activation

The activation background was measured during the irradiation inside the target room and after using the detectors themselves and a LN cooled GMX series coaxial HPGe detector. Fig. 7 shows the pulse-height spectra measured with one of the CZT detectors before and during proton irradiations and after 2 weeks of cool-down. Spectrum 1 was taken inside the target room before irradiation. The only peak seen in this spectrum is the 511-keV gamma line from the external background inside the target room. Spectra 2 and 3 were collected between exposing the detectors to the fluences of 1.2×10^7 and 3.9×10^7 p/cm^2, respectively. Spectrum 4 was acquired after exposure to the total fluence of 9×10^9 p/cm^2. The latter spectrum was taken 2 months after the irradiation. During that time, we carried out 2 runs of annealing to fully recover the detector performances. For comparison, Fig. 7 also shows the spectrum measured with the HPGe detector 2 weeks after irradiation. Some lines, seen in HPGe spectrum, became almost invisible in spectrum 4 measured 2 months later, because of the short-lived radionuclides decay. Conversely, the internal conversion electron lines in spectrum 4 are not seen in HPGe spectrum.

3.4. Detectors annealing

Following recipes described in [15–17], we annealed the detectors in a dry air environment to recover their performance. First, we annealed detectors for 3 weeks at the temperature of 65 degree C that had no effect on recovering the detector responses. After the 2 weeks annealing at 80 degree C (the temperature recommended by other researchers), the detectors recovered and showed the same energy resolution (after the interaction depth corrections) as before. However, the measured electron lifetimes were 58, 54, 58, and 49 μs, which is ~50%–60% of the original values. Fig. 8 shows the pulse-height spectra from ^{137}Cs after the annealing. To emphasize that the detector performances were not fully recovered we used the initial calibration parameters (before irradiation) to plot these spectra. As seen, the peak positions are left shifted by ~20 channels. Additional low-energy lines are due to internal activation.

The spectra in Fig. 8 were collected for over 2 months without interruptions while the detectors were continuously biased at 3700 V. The purpose of these measurements was to demonstrate the long-term detector stability after annealing, particularly the absence of the polarization reported by some groups. No shifts in the peak positions, which would indicate the polarization effect, were observed after 2 month of continuous data acquisition. Slight increases of the peak widths are due to small temperature variations with ~5 degree C in our lab.

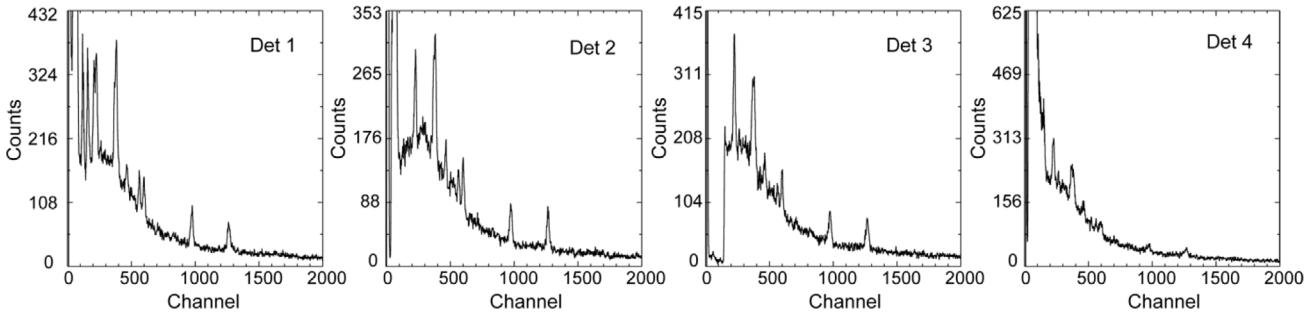

Fig. 6. Pulse-height spectra measured inside the target room after the detectors received a proton fluence of 10^7 p/cm^2. The majority of the gamma lines seen in the spectra are from external activation of the materials inside the target room.

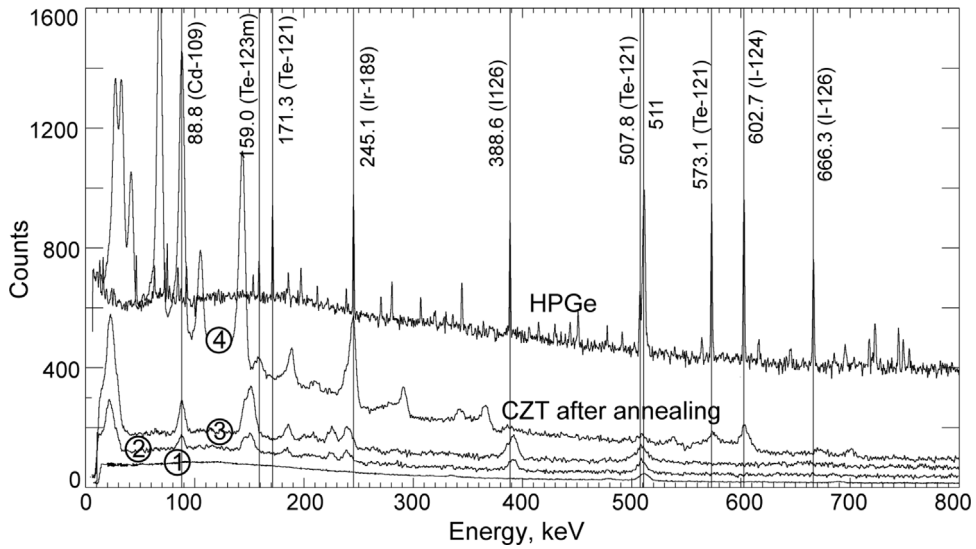

Fig. 7. The pulse-height spectra measured with one of the CZT detectors before and during proton irradiations, and after 2 weeks of the detectors cooling-down. Spectrum 1 was taken inside the target room before irradiation. The only peak seen in this spectrum is the 511-keV gamma line from the external background inside the target room. Spectra 2 and 3 were collected between exposing the detectors to fluences of 1.2×10^7 and 3.9×10^7 p/cm^2, correspondently. Spectrum 4 was acquired after exposure to the total fluence of 9×10^9 p/cm^2. The latter spectrum was taken ~2 months after the irradiation. The spectrum measured with the HPGe detector 2 weeks after irradiation is also shown.

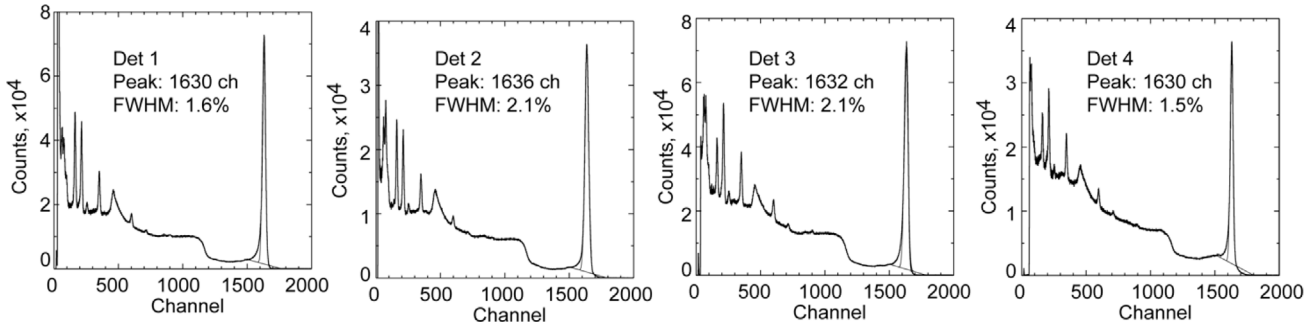

Fig. 8. The pulse-height spectra from ^{137}Cs after annealing. To emphasize that the detector performances were not fully recovered we used the initial calibration parameters (before irradiation) to plot these spectra. Additional low-energy lines are due to internal activation. We note the 20–30 channel shifts in the ^{137}Cs photopeak positions in comparison to the original spectra shown in Fig. 2.

After completing these measurements, the detectors were stored in a dry air environment and remained unused for a year. After a year, we retested the detectors (to verify that nothing changed in their performance) and carried out the third 2-week annealing which resulted in full recovery of the detector electron lifetimes and improving their performances. The measured electron lifetimes were 84, 77, 83, and 71 μs. We did not observe any activation lines in the pulse-height spectra. Also, we noticed reductions in leakage currents and electronic noises, particularly at high voltages. As an example, Fig. 9 shows ^{137}Cs spectra measured after the second annealing.

4. Conclusions

We have investigated the feasibility of using arrays of long-drift large-volume CZT detectors in space telescopes operating in low Earth orbits. We employed the proton beam at the NASA Space Radiation Laboratory with energies of 100 and 150 MeV to irradiate 4 8x8x32 mm^3 detectors. No polarization effects were observed as the detectors were irradiated by protons with fluxes up to 160 p/cm^2/s for several hours. We observed small (<2%) shifts of the peak positions after proton exposure up to 4×10^7 p/cm^2 due to radiation damage, which can

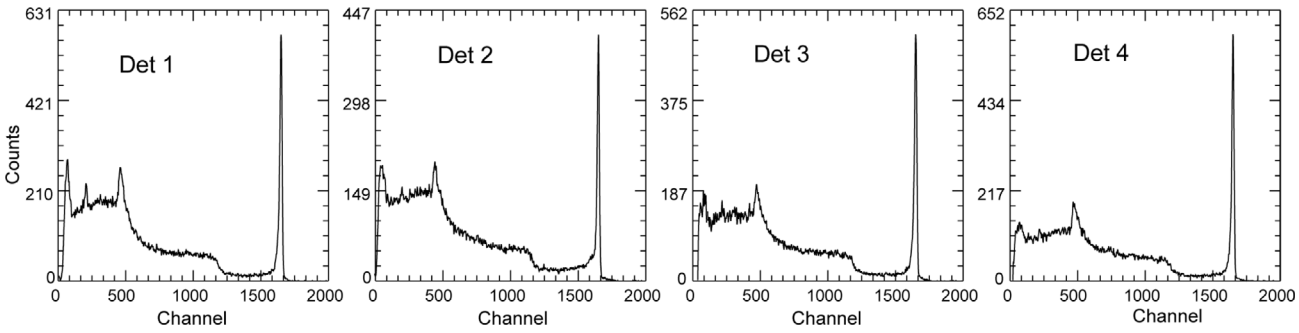

Fig. 9. 1D corrected ^{137}Cs spectra measured after the third annealing. The energy resolution was found to be in the range 1.2–1.4% FWHM at 662 keV and the interaction depth correction.

be corrected using in orbit calibrations. Such a radiation dose could be expected during a 5-year mission. The detectors stopped responding to gamma radiation completely after receiving the extremely high dose of ~10^{10} p/cm^2. However, after two annealing cycles (at 80 degree C for 3 weeks) their performances were fully recovered. We are planning to investigate in the future if the performance recovery level has been reached in shorter time.

The internal background of the activated CZT detectors poses another problem affecting the sensitivity of space telescopes. We measured the activation spectra in CZT detectors after exposure to different proton fluences, up to 10^{10} p/cm^2. Most of the observed gamma ray lines were from the short-lived radionuclide decays. These lines became practically invisible after 10 months after exposure. We are planning a more systematic study of large-volume CZT detector activation using both protons and neutrons to assess the potential radiation induced effects in LEO and response recovery steps.

CRediT authorship contribution statement

A. Bolotnikov: Conceptualization, Investigation, Writing – original draft. **G. Carini:** Supervision. **M. Chekhlov:** Data analysis. **A. Dellapenna:** Investigation. **J. Fried:** Investigation. **J. Haupt:** Investigation. **S. Herrmann:** Investigation. **I. Kotov:** Investigation. **D. Medvedev:** Spectroscopic measurements, Investigation. **A. Moiseev:** Supervision, Conceptualization. **G. Pinaroli:** Investigation. **A. Rusek:** Experimental facility operation. **M. Sasaki:** Investigation. **M. Sivertz:** Experimental facility operation. **L. Smith:** Data visualization. **E. Yates:** Software, Manuscript editing.

Declaration of competing interest

The authors declare that they have no known competing financial interests or personal relationships that could have appeared to influence the work reported in this paper.

Acknowledgments

This work was supported by the U. S. Department of Energy, Office of Defense Nuclear Nonproliferation Research & Development (DNN R&D). The manuscript has been authored by Brookhaven Science Associates, LLC under Contract No. DE-SC0012704 with the U. S. Department of Energy. The efforts of A. Moiseev and M. Sasaki are supported by NASA, USA awards 80GSFC21M0002 and 80NSSC20K057. The efforts of E. Yates and L. Smith are supported by NASA, USA award 80NSSC20K057

References

[1] J. McEnery, et al., All-sky medium energy Gamma-ray observatory AMEGO: Exploring the extreme multimessenger universe, Bull. Am. Astron. Soc. 51 (2019) 245.
[2] A.A. Moiseev, et al., New mission concept: Galactic Explorer with a Coded Aperture Mask Compton Telescope (GECCO), 2021 International Cosmic Ray Conference (Berlin, 2021), PoS (ICRC2021) 648.
[3] A.E. Bolotnikov, G.S. Camarda, G. De Geronimo, J. Fried, R.B. James, A 4x4 array module of position-sensitive virtual frisch-grid CdZnTe detectors for gamma-ray imaging spectrometers, Nucl. Instrum. Methods Phys. Res. 954 (2020) 161036.
[4] L.A. Franks, B.A. Brunett, R.W. Olsen, D.S. Walsh, G. Vizkelethy, J.I. Trombka, B.L. Doyle, R.B. James, Radiation damage in room temperature semiconductor radiation detectors, Nucl. Instrum. Methods Phys. Res. A 428 (1999) 95–101.
[5] B.D. Ramsey, Fine-pixel imaging CdZnTe arrays for space applications, in: 2001 IEEE Nuclear Science Symposium Conference Record, 4, 2001, pp. 2377–2381.
[6] G. Vedrenne, J.P. Roques, V. Schonfelder, P. Mandrou, G.G. Lichti, A. von Kienlin, B. Cordier, S. Schanne, J. Knödlseder, G. Skinner, P. Jean, F. Sanchez, P. Caraveo, B. Teegar-den, P. von Ballmoos, L. Bouchet, P. Paul, J. Matteson, S. Boggs, C. Wunderer, P. Leleux, G. Weidenspointner, P. Durouchoux, R. Diehl, A. Strong, M. Casse, M.A. Clair, Y. Andre, SPI Instrumental background characteristics, Astron. Astrophys. 411 (2003) L63.
[7] N. Simões, J.M. Maia, R.M. Curado da Silva, S. Ghithan, P. Crespo, S.J.C. do Carmo, Francisco. Alves, M. Moita, N. Auricchio, E. Caroli, Inflight proton activation and damage on a CdTe detection plane, Nucl. Instrum. Methods Phys. Res. A 877 (2018) 183–191.
[8] O. Limousin, D. Renaud, B. Horeau, S. Dubos, P. Laurent, F. Lebrun, R. Chipaux, C. Boatella Polo, R. Marcinkowski d, M. Kawaharada e, S. Watanabe, M. Ohta, G. Sato, T. Takahashi, Astro-h CdTe detectors proton irradiation at PIF, Nucl. Instrum. Methods Phys. Res. A 787 (2015) 328–335.
[9] P. Ubertini, F. Lebrun, G. Di Cocco, A. Bazzano, A.J. Bird, K. Broenstad, A. Goldwurm, G. La Rosa, C. Labanti, P. Laurent, I.F. Mirabel, E.M. Quadrini, B. Ramsey, V. Re-glero, L. Sabau, B. Sacco, R. Staubert, L. Vigroux, M.C. Weisskopf, A.A. Zdziarski, IBIS: THe imager on-board, Integr. Astron. Astrophys. 411 (2003) L131–L139.
[10] M. Martucci, R. Sparvoli, S. Bartocci, R. Battiston, W. Burger, D. Campana, L. Carfora, G. Castellini, L. Conti, A. Contin, C. De Donato, C. De Santis, F. Maria Follega, R. Iuppa, I. Lazzizzera, N. Marcelli, G. Masciantonio, M. Merge, A. Oliva, G. Osteria, F. Palma, F. Palmonari, B. Panico, A. Parmentier, F. Perfetto, P. Picozza, M. Piersanti, M. Pozzato, E. Ricci, M. Ricci, S. Bruno Ricciarini, Z. Sahnoun, V. Scotti, A. Sotgiu, V. Vitale, S. Zoffoli, P. Zuccon, Trapped proton fluxes estimation inside the south atlantic anomaly using the NASA AE9/AP9/SPM radiation models along the China seismo-electromagnetic satellite orbit, Appl. Sci. 11 (2021) 3465.
[11] NASA Space Radiation Laboratory. https://www.bnl.gov/accelerators/NSRL.php.
[12] A.E. Bolotnikov, J. MacKenzie, E. Chen, F.J. Kumar, S. Taherion, G. Carini, G. De Geronimo, J. Fried, Kihyun Kim L. Ocampo Girado, E. Vernon, R.B. James, Performance of 8x8x32 and 10x10x32 mm3 CdZnTe position-sensitive virtual frisch-grid detectors for high-energy gamma-ray cameras, Nucl. Instrum. Methods Phys. Res. A 969 (2020) 164005.
[13] A.E. Bolotnikov, K. Ackley, G.S. Camarda, C. Cherches, Y. Cui, G. De Geronimo, J. Fried, D. Hodges, A. Hossain, W. Lee, G. Mahler, M. Maritato, M. Petryk, U. Roy, C. Salwen, E. Vernon, G. Yang, R.B. James, An array of virtual frisch-grid CdZnTe detectors and a front-end application-specific integrated circuit for large-area position-sensitive gamma-ray cameras, Rev. Sci. Instrum. 86 (2015) 7.
[14] A.E. Bolotnikov, G.S. Camarda, E. Chen, Rubi. Gul, Vaclav. Dedic, Gianluigi. Geronimo, Jack. Fried, Anwar. Hossain, J. MacKenzie, L. Ocampo, P. Sellin, S. Taherion, E. Vernon, Ge. Yang, Uri. El-hanany, R.B. James, Use of the drift-time

method to measure the electron lifetime in long-drift-length CdZnTe detectors, J. Appl. Phys. 120 (2016) 104507.

[15] B. Fraboni, A. Cavallini, N. Auricchio, W. Dusi, M. Zanarini, P. Siffert, Recovery of radiation damage in CdTe and CdZnTe detectors, in: IEEE Symposium Conference Record Nuclear Science, 2004, pp. 4312–4317.

[16] J. Xia, Interaction Reconstruction in Digital 3-D CdZnTe Under Various Circumstances, Ph. D. Thesis, University of Michigan, 2019.

[17] S.A. Abraham, Y. Zhu, J. Xia, Z. He, Performance of neutron-damaged 3-D position sensitive CdZnTe detectors, in: Presented At the 2020 Nuclear Science Symposium and Medical Imaging Conference.